A new perfusion culture method with a self-organized capillary network

AUTHOR(S):

Sugihara, Kei; Yamaguchi, Yoshimi; Usui, Shiori; Nashimoto, Yuji; Hanada, Sanshiro; Kiyokawa, Etsuko; Uemura, Akiyoshi; Yokokawa, Ryuji; Nishiyama, Koichi; Miura, Takashi

CITATION:

Sugihara, Kei ...[et al]. A new perfusion culture method with a self-organized capillary network. PLOS ONE 2020, 15(10): e0240552.

ISSUE DATE:

2020-10-28

URL:

http://hdl.handle.net/2433/261994

PLOS ONE

RESEARCH ARTICLE

A new perfusion culture method with a self-organized capillary network

Kei Sugihara[1], Yoshimi Yamaguchi[1], Shiori Usui[1], Yuji Nashimoto[2,3,4], Sanshiro Hanada[5], Etsuko Kiyokawa[6], Akiyoshi Uemura[7], Ryuji Yokokawa[4], Koichi Nishiyama[5], Takashi Miura[1]*

1 Department of Anatomy and Cell Biology, Kyushu University Graduate School of Medical Sciences, Fukuoka, Japan, **2** Frontier Research Institute for Interdisciplinary Sciences (FRIS), Tohoku University, Miyagi, Japan, **3** Graduate School of Engineering, Tohoku University, Miyagi, Japan, **4** Department of Micro Engineering, Kyoto University, Kyoto, Japan, **5** International Research Center for Medical Sciences (IRCMS), Kumamoto University, Kumamoto, Japan, **6** Department of Oncologic Pathology, Kanazawa Medical University, Ishikawa, Japan, **7** Department of Retinal Vascular Biology, Nagoya City University Graduate School of Medical Sciences, Aichi, Japan

* miura_t@anat1.med.kyushu-u.ac.jp

OPEN ACCESS

Citation: Sugihara K, Yamaguchi Y, Usui S, Nashimoto Y, Hanada S, Kiyokawa E, et al. (2020) A new perfusion culture method with a self-organized capillary network. PLoS ONE 15(10): e0240552. https://doi.org/10.1371/journal.pone.0240552

Editor: Roeland M.H. Merks, Universiteit Leiden, NETHERLANDS

Received: May 12, 2020

Accepted: September 28, 2020

Published: October 28, 2020

Data Availability Statement: All relevant data are within the manuscript and its Supporting Information files.

Funding: This work was financially supported by JST CREST (Grant Number JPMJCR14W4).

Competing interests: The authors have declared that no competing interests exist.

Abstract

A lack of perfusion has been one of the most significant obstacles for three-dimensional culture systems of organoids and embryonic tissues. Here, we developed a simple and reliable method to implement a perfusable capillary network in vitro. The method employed the self-organization of endothelial cells to generate a capillary network and a static pressure difference for culture medium circulation, which can be easily introduced to standard biological laboratories and enables long-term cultivation of vascular structures. Using this culture system, we perfused the lumen of the self-organized capillary network and observed a flow-induced vascular remodeling process, cell shape changes, and collective cell migration. We also observed an increase in cell proliferation around the self-organized vasculature induced by flow, indicating functional perfusion of the culture medium. We also reconstructed extravasation of tumor and inflammatory cells, and circulation inside spheroids including endothelial cells and human lung fibroblasts. In conclusion, this system is a promising tool to elucidate the mechanisms of various biological processes related to vascular flow.

Introduction

Multicellular pattern formation has been one of the central issues in developmental biology [1–3]. An extensively used tool to understand the mechanism of pattern formation is an organ culture system in which embryonic tissue is cultured at the air-liquid interface [4]. Recent advancements in stem cell biology have enabled the generation of small tissue structures from a single cell, which is called an organoid, and various organoids have been established [5].

A technical obstacle for standard culture systems of three-dimensional tissue structures is the lack of microcirculation. There are various methods to improve oxygen supply, such as culture inserts and rotator culture [6]. However, these methods cannot overcome the size limitation, i.e., if the cultured tissue size exceeds a 100-μm order, the tissue undergoes necrosis due

to hypoxia [7]. Organ culture system of embryonic tissue with functional capillary network has not been established yet. For example, the tube formation assay has been classically used to assess the pattern formation capability of endothelial cells [8], but the generated network structure lacks a functional lumen and is not perfusable.

Interactions between vascular endothelial cells and other types of cells are one of the main themes of study in vascular biology. A major example is pericytes that exist between basement membranes of endothelial cells, which stabilize the biological activities of the endothelial cells [9]. In addition, endothelial cells interact with circulating cells in blood [10]. For example, neutrophils transmigrate through endothelial cells at an inflammation site [11]. In cancer biology, hematogenous metastasis involves adhesion of tumor cells to endothelial cells and invasion [12].

In tissue engineering, various methods have been developed to implement a capillary network in a microfluidic device for perfusion in culture systems [13]. These methods are classified into two categories: predesigned and self-organization methods. Predesigned methods align endothelial cells by engineering techniques. Self-organization methods employ the spontaneous pattern formation capacity of cells to generate capillary network structures (reviewed in [6]). Recent advances in the integrative studies of tissue engineering and vascular biology have enabled construction of a perfusable vascular network in vitro. For example, in 2013, a microfluidic device was developed with a self-organized perfusable vascular network [14]. We have previously integrated a spheroid culture system with the self-organized capillary network to improve the culture conditions of spheroids [15, 16]. Roger Kamm group have provided various on-chip vascular models to examine the tumor metastasis and interaction with immune cells [17–19].

Currently, these new culture methods are highly technical and difficult to implement in a common biological laboratory. Various microfluidic chips are commercially available [20], but collaboration with engineering researchers is needed to obtain microfluidic devices with optimized designs. For perfusion itself, syringe pumps are not very common in a biological laboratory, and it is still technically difficult to connect tubes without collapsing the capillary network in a gel.

In the present study, we developed an easy method to enable microcirculation in ordinary glass-bottom culture dishes. We developed a culture system to perfuse culture medium in the lumen. Although the pressure difference is not constant, the flow persisted for 12–24 hours per one medium change, enabling long-term perfusion. We observed the main features of the endothelial pattern formation, which correlated with flow, endothelial cell shape changes, collective migration towards the upstream of the flow, remodeling of the vascular network, extravasation of tumor cells, the effect of pericytes on pattern formation, and the perfusion of vascularized spheroids. These results show the usefulness of this culture method for elucidating various biological phenomena.

Materials and methods

Cell culture

We used commercially available human umbilical vein endothelial cells (HUVECs) to generate a perfusable vascular network based on a previous report [14]. We used optimized growth media supplied by Lonza Inc. to maintain these cells. We used LFs for the coculture system [21], which were maintained using FGM-2 culture medium and protocols provided by the manufacturer (Lonza Inc.). For visualization purposes, we used red fluorescent protein (RFP)-labeled HUVECs and GFP-labeled human placental microvascular pericytes (cAP-0029GFP) from Angio-proteomie Inc. HL60 and NMuMG-Fucci cells were provided by the Riken

Bioresource Research Center (RCB2813 and RCB0041, respectively). Colon Tumor 26 (C26) is a colon cancer cell line isolated from a BALB/c mouse treated with carcinogen *N*-nitroso-*N*-methylurethan [22]. C26 cells were injected into the spleen, and cells that metastasized to the liver were isolated. By repeating this injection-isolation cycle four times, LM4 cells were isolated. The details of LM4 cells will be described elsewhere (EK, manuscript in preparation). HL-60 and LM4-GFP cells were maintained in RPMI 1640 medium (Nacalai Tesque, Inc.) supplemented with 10% FBS and 1% penicillin-streptomycin.

Culture dishes

We developed a culture dish to exert static pressure on the self-organized capillary system. This dish consisted of standard 35- or 60-mm glass-bottom tissue culture dishes with a glass separator. Glass separators were prepared by cutting slide glass (Matsunami, 24 x 50 mm, No. 1, 0.12–0.17mm thickness) into 35mm x 7mm pieces with glass cutter (NC-X03). The 12 phi glass well part was left open (Fig 1A). This type of dish was obtained from a local manufacturer or assembled using a glass coverslip and bioinert adhesive such as replisil (silicone).

Generation of a self-organized vascular network

In the first protocol, endothelial cells generated a capillary network by self-organization and the culture medium was perfused into the network by static pressure. First, we prepared 5.0×10^6 HUVECs per 1.5ml Eppendorf tube, centrifuged the tubes (1000 rpm, 5 min, RT), and removed the culture medium. Then we added 150 μl of fibrin/collagen gel solution (5 mg/ml fibrin, 0.2 mg/ml type I collagen (rat tail, Enzo Life Sciences Inc., Alx-522-435-0020), and 0.15 U/ml aprotinin) per one tube and resuspended the cells. Finally, we added 1 μl of 0.5 U/ml thrombin per one tube and quickly poured the fibrin/collagen/HUVEC solution into the well to separate the left and right halves of the dish divided by a glass separator. For HUVEC-pericyte experiment (Fig 5), pericytes (Angio-proteomie cAP-0029GFP) were cultivated according to the manufacturer's protocol, and mixed to HUVEC-fibrin suspension (5.0×10^4 cells / dish).

The dishes were incubated for 5 min at room temperature and then for 1 h at 37 ^{o}C to solidify the fibrin gel. Then, we added 5×10^5 LFs in a 5 mg/ml fibrin gel solution (100 μl volume) at the edge of a 35-mm culture dish to avoid physical contact of LFs and HUVECs. The dishes were incubated again for 1 h at 37 ^{o}C to solidify the fibrin gel. Then, we added 1 ml EGM-2 with 10 μM tranexamic acid to each well of the culture dish (total amount: 2 ml) and incubated the dish for 7 days. There existed a considerable difference in lumen formation capacity among a different lot of HUVECs. Depending on the HUVEC activity, the culture period may be shorter. Culture media were changed once every 2–3 days. After confirmation of capillary network formation with lumens, we cut the edge of the preformed network using tungsten needles or a sharp scalpel to make open ends (We defined the location of cut with culture medium as an inlet (where the culture medium flowed into the capillary network) and the cut of the other side of dish as an outlet (where the culture medium flows out of the capillary network)). We put the needle or knife blades perpendicular to the gel surfaces, and then due to the surface tension, the small opening of the gel appears. Then, we removed the culture medium from both wells and added 1 ml of culture medium to one of the wells. After the culture period, a small opening remained (S2A Fig), and the walls of the openings were bordered by the endothelial cells and formed a stable channel (S2B–S2D Fig, arrows). The existence of flow in the vascular network was confirmed by the flow of cell debris during the long-term culture (S3 Movie). Depending on the flow resistance, the water level difference persisted up to 24 hours. A common cause of failure at this point is the leak at the separator level. In which case,

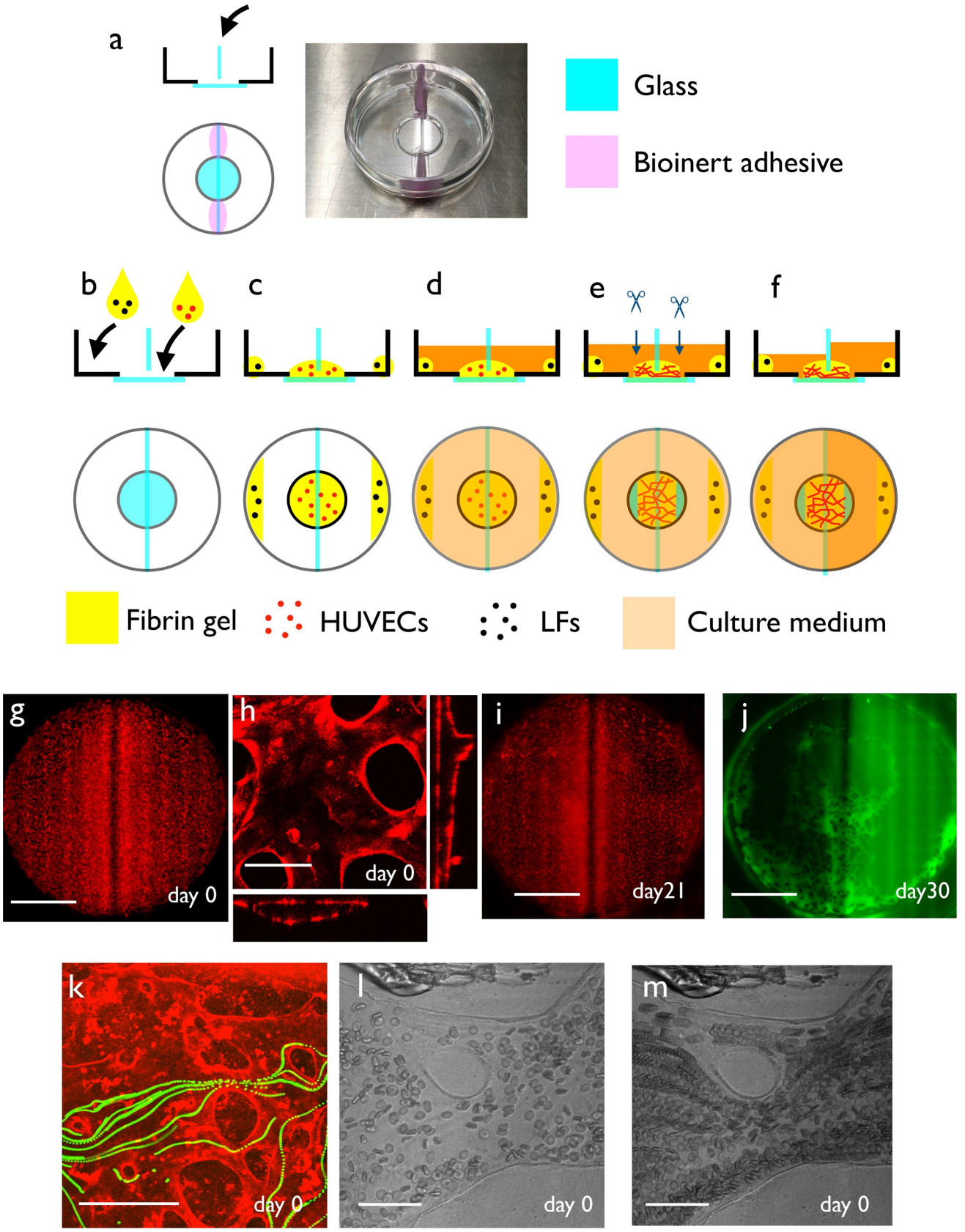

Fig 1. Culture system setup. (a) Side and top views of the culture dish before setup. The dish was a normal 12-phi glass-bottom dish. A glass separator was set at the center of the dish with a bioinert adhesive. (b) First, we placed 150 μl fibrin gel mixed with HUVECs in the center of the glass plate, so that two sides of the dish were separated by the glass separator and fibrin gel. We also added LF-containing fibrin gel at the edge of the dish. (c) We incubated the dish for 30 min to solidify the fibrin gel. (d) We added 1 ml culture medium to both wells and incubated the dish for 1 week. (e) After 1 week of culture, a vascular network with a perfusable lumen was formed in the glass-bottom region. Then, we cut both edges of the regions to make openings. (f) After the cuts, we increased the amount of culture medium on one side of the dish. This caused a static pressure difference between both openings of the self-organized capillary network, resulting in steady flow inside the apparatus. (g) Low magnification view of the self-organized vascular network. RFP-HUVECs were cultivated in the fibrin gel, and we observed the vascular network formation. (h) High magnification view of (g). Vascular network with a lumen was generated in the fibrin gel region. (i) Low magnification view of the self-organized vascular network after long-term culture with flow. (j) Visualization of the perfusable area by FITC-dextran. Perfusable regions existed near the inlet and outlet, near the glass separator and edge of the well. (k) Flow inside the lumen was visualized using fluorescent beads. (l) Snapshot of the culture system when using whole blood as a tracer. Red blood cells were flowing inside the self-organized vasculature. (m) Projection of multiple frames of (l). Movements of red blood cells were visualized as a stream. Scale bars: 3 mm (g, i, j); 100 μm (h); 500 μm (k); 50 μm (l, m).

https://doi.org/10.1371/journal.pone.0240552.g001

the water level difference quickly disappeared within several minutes. To prevent this trouble, we need to use enough amount of adhesive and fibrin gel.

Observation of vascular extravasation of neutrophils and tumor cells

Neutrophil-like differentiated HL-60 (dHL-60) cells were prepared by treating HL-60 cells with 1.25% DMSO (Nacalai Tesque, Inc.) for 2 days. To facilitate the lumen formation (S1J Fig), two pieces of thin PDMS sheet of roughly 6–8 mm in size were placed on the glass bottom in parallel to each other and perpendicular to the glass separator before applying the HUVEC-containing fibrin gel. HL-60 and dHL-60 cells were visualized with CellTracker Green CMFDA (1:1000, Thermo Fisher Scientific). Then, 4×10^6 HL-60, 1×10^6 dHL-60, or 1×10^6 LM4-GFP cells were suspended in 2 mL EGM-2 and applied to one side of the dish. For endothelial activation, 10 ng/mL human recombinant TNF-α (PeproTech, Inc.) was added to the medium overnight before the experiment. The HUVEC vascular network was visualized by incubation with rhodamine-conjugated UEA-I lectin (1:1000, Vector Laboratories) for 60 minutes in advance. Time-lapse and z-stack observations were performed with a Nikon A1R microscope.

Generation of perfusable spheroids with vasculature

We also developed a protocol to perfuse spheroids with an endothelial cell vasculature (Fig 8A). First, we prepared spheroids containing lung fibroblast and endothelial cells, and embedded the spheroid in a 2-well dish with fibrin gel. After the spheroids sprouted, we cut the tip of the sprout with a sharp scalpel and exerted static pressure for perfusion. Detail of the protocol is described below.

First, we prepared HUVECs, target cells, and lung fibroblasts. Then, we mixed HUVECs, lung fibroblasts, and target cells in a Sumiron MS-9096U 96-well dish. The ratio of HUVECs: LFs:target cells was 40:10:4. We cultivated the spheroids for 2 days.

Next, we embedded spheroids in the culture dish. We prepared the culture dish, fibrin, and thrombin solution. The culture dish was cooled on ice. We collected the spheroids in a 1.5-ml Eppendorf tube and removed the supernatants. Next, we added 150 μl of the fibrin gel solution to the Eppendorf tube on ice. Then, we added 1 μl of the thrombin solution to the Eppendorf tube, quickly agitated the spheroids, and then transferred the solution to the 2-well dish. We moved the dish to the stage of an inverted microscope (×2 objective lens) and carefully adjusted the locations of the spheroids using tungsten needles. The fibrin gel was solidified for 5 min at room temperature and then for 1 hour at 37˚C. During this period, we prepared LFs mixed with the fibrin gel solution. Finally, we added the thrombin solution to the LF-fibrin solution and then transferred the LF-fibrin gel solution to the side of the 2-well dish. After the fibrin gel solidified for 1 hour at 37˚C, we added 2 ml EGM-2 with 10 μM tranexamic acid and

incubated the dishes for 7 days for the sprouts to elongate. Finally, we seeded HUVECs on the solidified fibrin gel to prevent leak. Culture media were changed once every 2–3 days.

Flow tracers

We used various flow and permeability tracers to observe the characteristics of flow. (1) To show actual hemocytes could go through the network, we used diluted whole blood as a tracer. Whole blood from a volunteer was diluted 10-fold with the EGM-2 culture medium to observe the capillary network's red blood cell perfusion in the brightfield image. (2) To measure the velocity of flow, fluorescent particles (5 μm, Duke Scientific G0500) were used. (3) To assess the flow and vascular permeability, and to confirm there is no leak in the generated vascular network, FITC-dextran (70 kDa) was used.

Histology and immunohistochemistry

Cultured blood vessels and spheroids were fixed in 4% PFA (immunohistochemistry) or Bouin's fixative (HE staining) overnight. Fixed specimens were dehydrated using 70% ethanol in situ, detached from the culture dish, and transferred to a glass bottle. The samples were further dehydrated in graded concentrations of ethanol. Then, the ethanol was substituted with xylene and paraffin. The paraffin block was cut at 10 μm thicknesses. For histology, these sections were stained with hematoxylin and eosin.

For immunohistochemistry and terminal deoxynucleotidyl transferase dUTP nick end labeling (TUNEL), sections were deparaffinized and stained using the protocols provided by the manufacturers. Antibodies against PDGFB (Abcam, ab23914), type IV collagen (LSL, LB-0445), and desmin (LabVision, MS-376-S0) were used. To detect apoptotic cells, we used an In situ Apoptosis Detection Kit (Takara Bio, MK500).

Image acquisition and analysis

Observation of three-dimensional structures was conducted using a Nikon A1R confocal microscope. For long-term observation of the whole culture dish, we used a Keyence BZ-900 with a tiling function. All image analysis was performed using ImageJ [23] or Fiji [24]. To observe vessel wall movement in long-term culture, we used the "linear stack alignment with SIFT" plugin for registration of the figures obtained at various time points. We used the "Reslice" command to prepare kymographs of cell movements from time-lapse movies.

Results

Method for culture medium perfusion

We developed a culture method to perfuse the self-organized network in a glass-bottom dish. Using the protocol described in the Materials & Methods, we induced flow in the self-organized capillary network (Fig 1A–1D). After one week, the vascular network with a lumen was generated spontaneously (Fig 1E, 1G–1J). Then, we removed the culture medium from both wells and added culture medium (and tracer) to one of the wells (Fig 1F). If the lumens were connected, we observed flow using the various tracers. We applied fluorescent beads to detect the perfusability of the capillary network (S1 Movie, Fig 1K). However, the fluorescent beads adhered to the endothelial cell surfaces and interfered with the fluorescence observation. Therefore, this method was used only once per experiment. When whole blood diluted with EGM-2 was loaded, we observed the flow of red blood cells in the self-organized capillary network (S2 Movie, Fig 1L and 1M). The flow can persist for several hours, depending on the size of the cut. Since the amount of reservoir medium is limited, the flow rate and pressure difference are not constant during long-term perfusion.

Formation of a lumen around a solid object

In this culture system, we observed that lumen formation took place close to 'hard objects' such as the culture well wall and the glass separator (Fig 1J). Thick, perfusable lumens were formed in the region at 1 mm around the culture well wall or separating glass plate. This was not due to the high cell density around the periphery of the dish because increased cell density did not induce lumen formation in the center of the dish (S1A–S1D Fig). To test whether we could induce lumen formation close to hard objects, we embedded glass beads into the matrix. We observed lumen formation by embedding hard objects like glass beads in the gel. When we mixed glass beads (1 mm diameter) with HUVECs at the beginning of the culture and cultivated the cells for 120 hours, we observed lumen formation around the glass beads (S1E–S1I Fig).

Flow-induced collective cell migration and cell shape changes in the culture system

In this system, we observed the dynamics of endothelial cells in response to flow (Fig 2). It is known that, at a certain range of flow rate, endothelial cells migrate collectively toward the upstream of blood flow [25–27]. We easily observed this phenomenon in our culture system. We used Hoechst 33342 as a vital stain of endothelial cell nuclei and exerted flow to a 35-mm culture dish. We then drew kymograph of flow and non-flow regions and observed the collective upstream movement of endothelial cells (S4 Movie, Fig 2A–2C). In the region with flow, the cells migrated collectively toward the direction of the dashed yellow arrow, which is the opposite direction as the flow exerted to the culture (Fig 2B). The white arrow indicates the orbit of cell debris, which should follow the flow direction. The comparison of these two orbits confirmed that the direction of cell movement was opposite to that of the flow. In contrast, only random movement of cells was observed in the non-flow region (Fig 2C), indicating that this system is useful to assess flow-endothelial cell interactions.

We next observed endothelial cell shape changes induced by the flow. After the culture period, we applied FITC-Dextran as a flow tracer and observed flow velocity. In the fast flow region, endothelial cells became elongated parallel to the direction of flow (Fig 2D–2G). In the slow flow region, the endothelial cells remained unpolarized (Fig 2H–2K). In the non-flow region, the endothelial cells formed isolated cysts with cell debris inside (Fig 2L–2N).

Reconstruction of vascular remodeling by long-term flow in the vasculogenesis system

Because flow could be slow depending on the geometry of vasculature and the size of the cut, we maintained the flow for a long time. As the reservoir medium decreased, the pressure gradient changed. In general, we could maintain flow for 24 hours, which allowed long-term flow effects. We confirmed the flow by observing the flow of cell debris in the brightfield view (S3 Movie). Unlike a two-dimensional culture system, HUVECs could be maintained for a very long period of up to 1 month without degradation of the fibrin gel (Fig 1I and 1J). The openings remained unobstructed after 3 weeks of culture (S2 Fig). A high magnification view revealed the occurrence of the remodeling process (Fig 3A and 3B). In the region with flow, the radius of the vascular segment was increased gradually (Fig 3A and 3A', S5 Movie). In the region without flow, the vasculature was degraded gradually and finally became fragmented vascular cysts (Fig 3B and 3B', S6 Movie).

Histological observation confirmed the remodeling process in this culture system. The surface of the fibrin gel was covered with HUVECs (Fig 3C and 3D). The flow region was covered by a relatively thick HUVEC sheet (Fig 3C and 3E). The non-flow region contained several

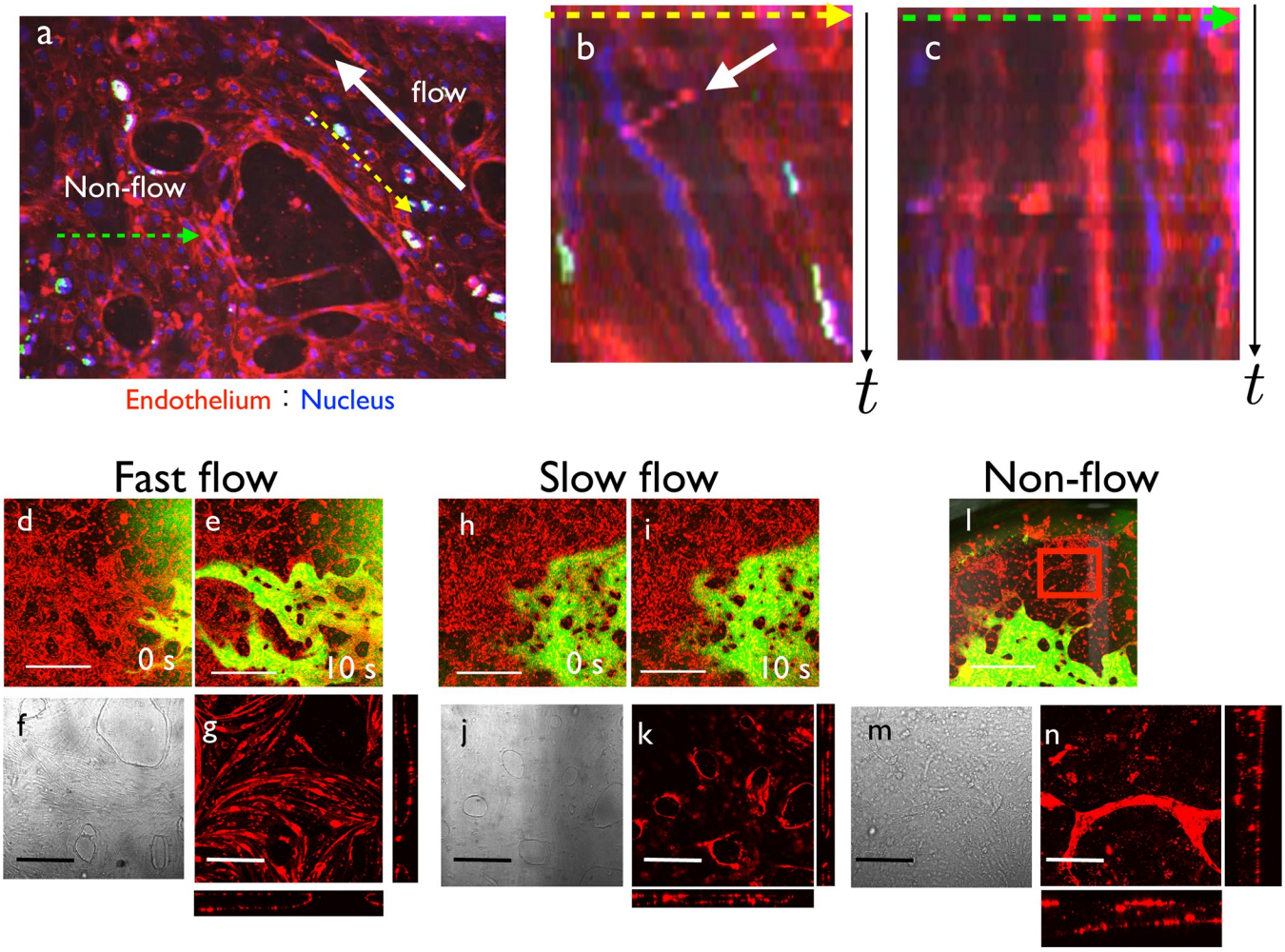

Fig 2. Flow-induced collective cell migration and cell shape changes. (a) Initial shape of the vascular network. HUVECs were stained with UEA1 and nuclei were stained with Hoechst 33342. There was a flow-positive region (yellow-dashed line) and non-flow region (green-dashed line). Direction of flow is indicated by a white allow. (b) Kymograph of the yellow-dashed line region. Horizontal direction represents space, and vertical direction represents time. Collective movement toward upstream of the flow was observed. White arrow indicates the flow of cell debris. (c) Kymograph of the green-dashed line region. Cell movement was random. (d–n) Cell shape changes induced by flow: (d, e) Fast flow. When FITC dextran was perfused, the vessel regions near the inlet or outlet showed fast flow. (f) Brightfield view of the fast flow region. Endothelial cells became shaped as spindles aligned parallel to the flow direction. (g) Fluorescence view of the fast flow region. At the floor of the lumen, we observed spindle-shaped cells parallel to the flow direction. (h, i) Slow flow. When FITC dextran was perfused, the vessel regions far from the inlet or outlet showed slow flow. (j) Brightfield view and (k) confocal view of the slow flow region. Endothelial cells did not show any polarity. (l) Low magnification view of the non-flow region. (m) Brightfield view and (n) confocal view of the non-flow region. Vasculatures were disconnected and became thin endothelial cysts with cell debris inside. Scale bars: 1 mm (d, e, h, i, l); 200 μm (f, g, j, k, m, n).

https://doi.org/10.1371/journal.pone.0240552.g002

apoptotic bodies (Fig 3C and 3F). To confirm the distribution of cell death, we applied TUNEL staining. Positive signal was observed in the non-flow region (Fig 3G and 3H), confirming the histological observation. We also observed an extracellular matrix sheath in which the basement membrane remained, while endothelial cells were retracted in the non-flow region (Fig 3I). These observations supported that vascular remodeling occurred in this culture system.

Effect of vascular flow on cell proliferation

Because the physiological role of vascular flow is the transfer of oxygen and nutrients, we examined the effect of flow on cell proliferation outside the blood vessel. We used Fucci-

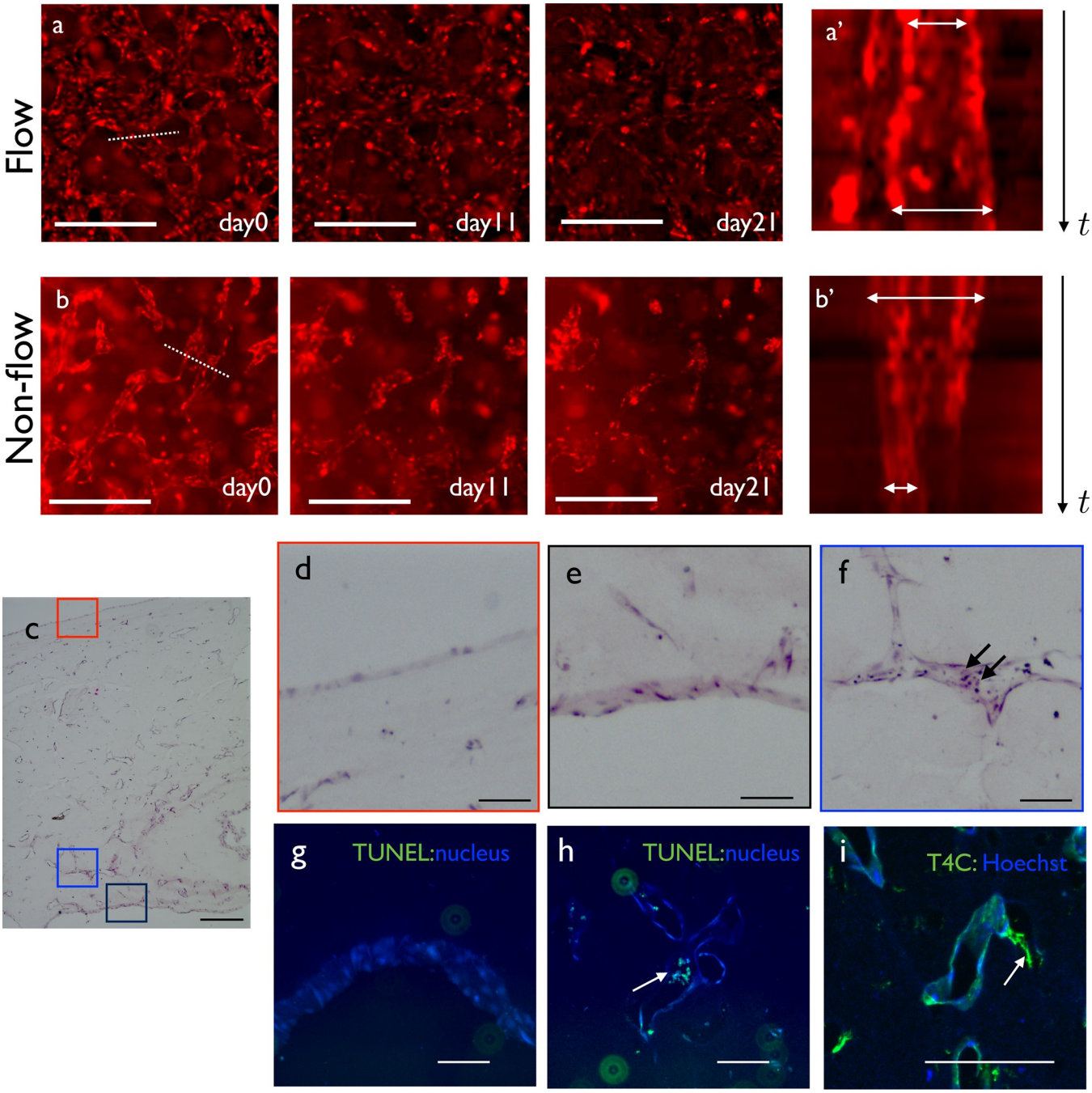

Fig 3. Reconstruction of flow-induced remodeling. (a) Remodeling process at the high flow region from day 0 to 21. (a') Kymograph of the dotted line region in (a). Vasculature dilated gradually. (b) Remodeling process at the non-flow region from day 0 to 21. (b') Kymograph of the dotted line region in (b). The vascular diameter decreased. (c) Low magnification view of a hematoxylin-eosin-stained EC monoculture sample. (d) Magnified view of the upper surface of the gel. The surface of the gel was covered by endothelial cells. (e) Magnified view of the large lumen inside the gel. The lumen was also covered by endothelial cells. (f) Magnified view of the small lumen inside the gel. Small necrotic cells were observed inside the lumen (arrows). (g) TUNEL staining of the flow region. No dead cells were observed. (h) TUNEL staining of the non-flow region. Dead cells were observed inside the vasculature. (i) Type IV collagen staining of the long-term culture sample. There were some lumens positive for type IV collagen without cells (arrows), indicating the ECM sheath of the degraded vasculatures in non-flow regions. Scale bars: 500 μm (a–c); 100 μm (d–i).

https://doi.org/10.1371/journal.pone.0240552.g003

containing NMuMG cells, with which we could dynamically observe the mitotic cells, to easily assess the effect of oxygen-nutrient transport by the flow on the mesenchyme region. In Fucci reporter containing cells, nuclei in S/G2/M phase become green while nuclei in G1 phase becomes red [28]. NMuMG cells were mixed with RFP-HUVEC suspensions and cultivated for one week (Fig 4A). Next, we made a cut to the network, and exert static pressure on only one group of the samples (Fig 4A). The NMuMG cells at the beginning of the experiments formed sparse colonies in the region away from the vasculature (Fig 4B). We then compared the GFP-positive area, which should reflect the proliferating cells in flow and non-flow samples and detected increased fluorescence by exerting flow (Fig 4C). The difference was most evident on day 1, possibly because the culture medium's effect started to diminish after 24 hours (Fig 4D). We detected a statistically significant difference between flow and non-flow samples at day 1, indicating that the medium perfusion improves cell cycle progression of cells in the vicinity of the perfused vasculature.

Dynamics of pericytes in the self-organized vascular network

Pericytes reside around endothelial cells and modulate their biological functions [9]. It has been reported that pericytes play an important role in the vascular remodeling process to generate a hierarchical vascular tree structure in developing retina [29]. To examine whether addition of pericytes to this culture system affected the remodeling process, we cocultured pericytes in this culture system and observed the long-term pattern change with flow. Vasculature with pericytes grew normally, and we maintained the culture system with pericytes for up to 1 month (S3A and S3B Fig). After 1 month, the vasculature was still perfusable without leak (S3C and S3D Fig). The morphology of vasculatures with pericytes was similar to that without pericytes (S3C and S3D Fig).

Interestingly, pericytes disappeared around the fast flow region and surrounded the endothelial vasculature in the non-flow region (Fig 5A and 5B). Initially, pericytes were distributed evenly (Fig 5A). After 3 weeks of culture, spots of high pericyte cell density appeared in non-flow regions (Fig 5B, arrows). However, in the fast flow region, the pericytes had disappeared (Fig 5B, red circle). We observed active migration away from the fast flow region (Fig 5C and 5D, S7 Movie). In the fast flow region, a very small number of pericytes was observed (Fig 5E). At the interface between flow and non-flow regions, we observed an increase of pericytes only in the non-flow region (Fig 5F). In the non-flow region, we observed pericytes wrapped around cysts of endothelial cells containing debris (Fig 5G). To understand this uneven distribution, we observed the protein distribution of PDGFB, a chemoattractant for pericytes (Fig 5H–5K). In the flow region, the PDGF immunohistochemical signal was low, while in the non-flow region, strong signals were detected in endothelial cell cysts and pericytes (Fig 5H–5K). This result suggested the higher level of PDGFB protein in the non-flow region might be one of the reasons why pericytes only remained in the non-flow region.

Reproducing extravasation of inflammatory cells from the capillary network

We next observed the interaction of blood cells and capillaries using this self-organization system. At first, we perfused fluorescent beads (Fig 1K) or red blood cells (Fig 1L and 1M) in the self-organized vascular network. We also perfused the neutrophil cell line HL-60 in the self-organized vascular network (Fig 6A and 6B, S8 Movie). We differentiated HL-60 cells by DMSO treatment and perfused the cell suspension in the self-organized vascular network. The cells had the ability to move through a very thin capillary segment (Fig 6C). We also observed the time course of extravasation (Fig 6D–6F). Three-dimensional observation confirmed that the HL-60 cells were outside of the vascular network (Fig 6G).

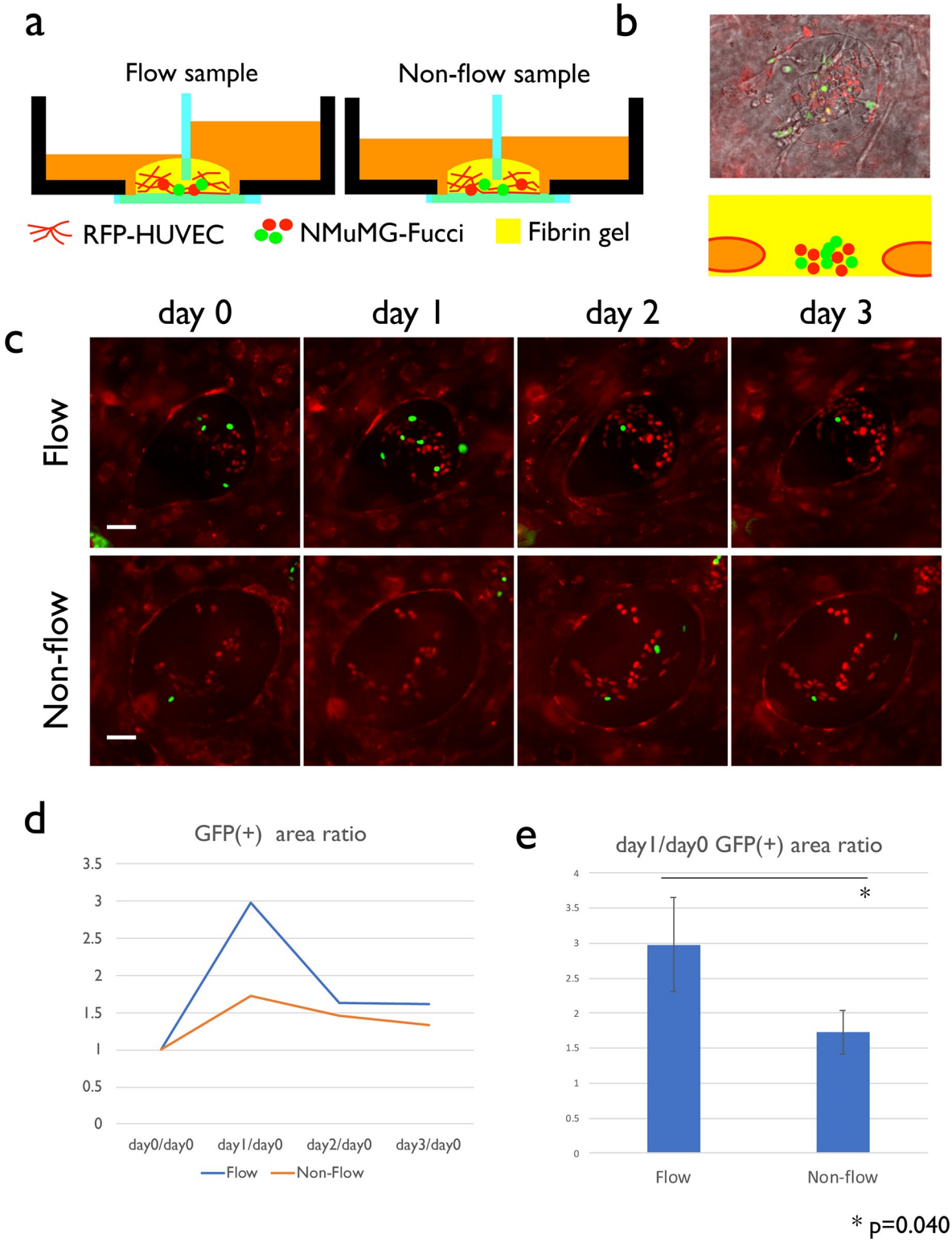

Fig 4. Effect of flow on cell proliferation. (a) Experiment setup. We prepared two groups of dishes in which a mixture of RFP-HUVECs and NMuMG-Fucci cells were seeded in the fibrin gel. After the perfusable network was formed, we made openings to both groups but transferred medium in only one group of the dishes. (b) Typical appearance of the NMuMG cell colony and its schematic representation. NMuMG-Fucci cells (red and green nuclei) forms colonies outside the vascular lumen. (c) Time course of the cell division monitored by Fucci reporter. (d) Time course of GFP(+) area ratio. 20 NMuMG-Fucci colonies were observed, and the area of GFP(+) areas was obtained using Fiji. (e) GFP(+) area ratio between day 1 and day 0. Statistically significant difference was detected (Student t-test). Scale bars: 50 μm.

https://doi.org/10.1371/journal.pone.0240552.g004

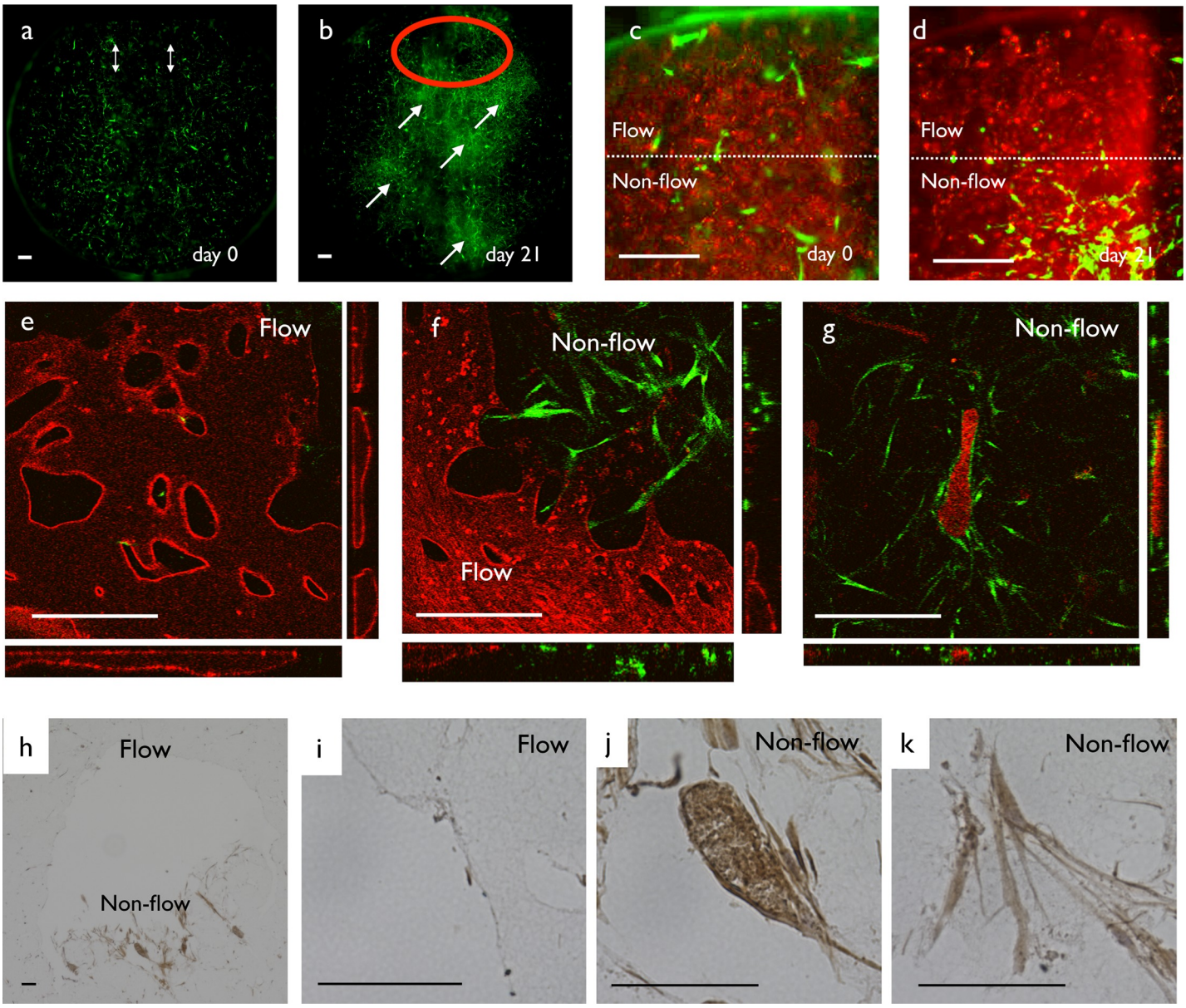

Fig 5. Dynamics of pericytes in the HUVEC-pericyte coculture system. (a) Low magnification view of the distribution of pericytes at day 0 (green). White arrows indicate the inlet and outlet. (b) Distribution of pericytes after 21 days of perfusion culture. We observed a high density region of pericytes (arrows) in the non-flow region and a low density region (red circle) in the flow region. (c) High magnification view of pericyte distribution at the flow region (day 0). (d) High magnification view of the pericyte distribution at the flow region (day 21). Pericyte cell density was decreased in flow region and increased in non-flow region. (e) 3D structure of the flow region at day 30. Endothelial cells (red) formed vasculature with a perfusable lumen. Pericytes were virtually absent. (f) Boundary between flow and non-flow regions. Pericytes resided in the non-flow region. (g) 3D structure of the non-flow region. Vasculature was degraded and flat cysts of endothelial cells with cell debris inside remained. Pericytes appeared to surround the degraded structure. (h) Low magnification view of PDGFBB immunohistochemistry. A positive signal was observed in the non-flow region. (i) High magnification view of the flow region. No positive signal was observed. (j) High magnification view of the non-flow region. The cell cyst and surrounding pericytes had a high staining intensity. (k) High magnification view of pericytes in the non-flow region. A positive signal was observed in the cytoplasm. Scale bars: 500 μm (a–g); 100 μm (h–k).

https://doi.org/10.1371/journal.pone.0240552.g005

Reproducing metastasis of cancer cells from capillary vessels

The other possible application of this culture system is assessment of hematogenous metastasis. We introduced the cancer cell line LM-4 into the culture medium with perfusion and observed the dynamics for up to 48 hours. As a result, the cells flowed inside the self-organized vascular

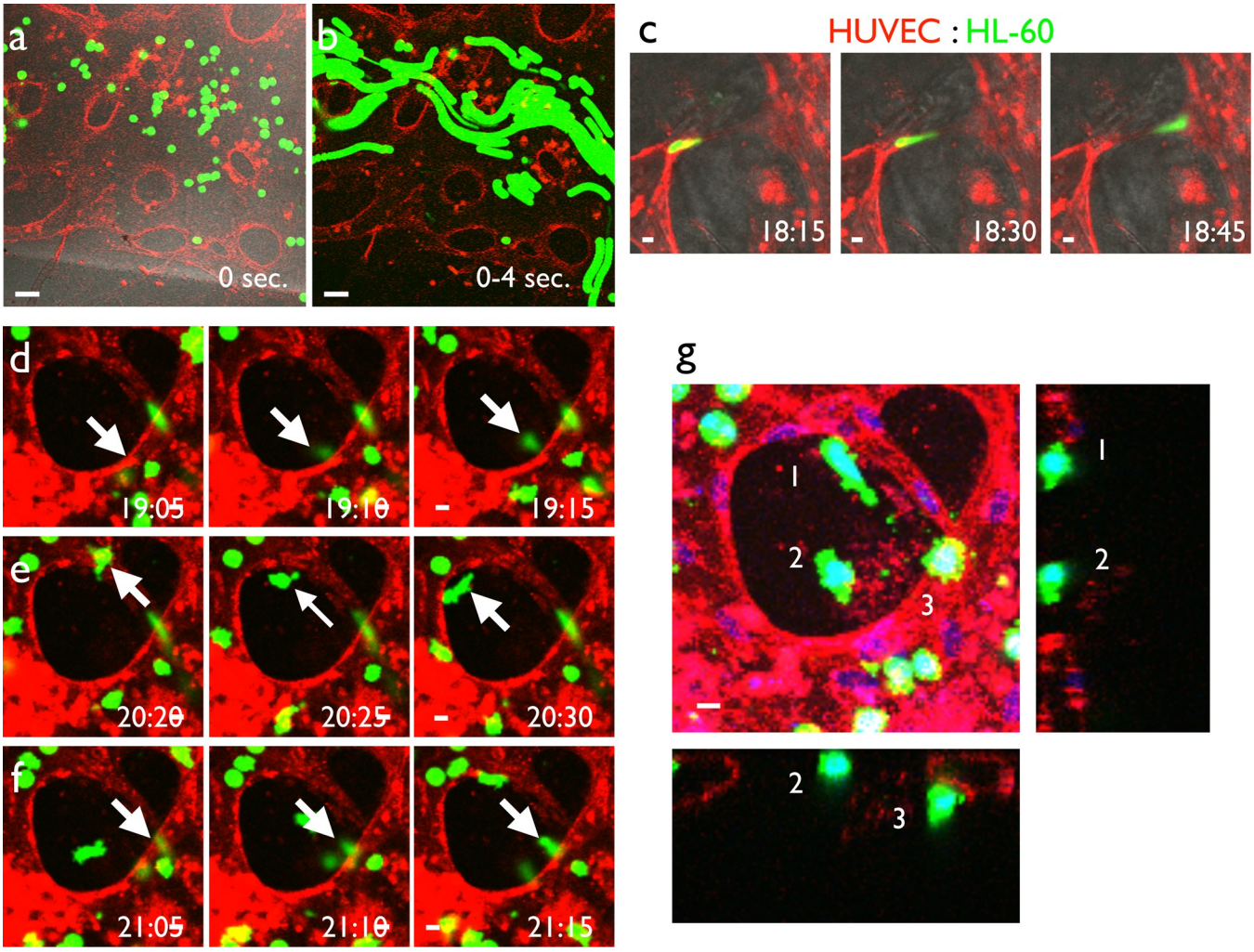

Fig 6. Extravasation of leukocytes using the self-organized vascular network. (a) HL-60 cells, an acute myelogenous leukemia cell line, were labeled with CellTracker Green and introduced into the self-organized vascular system visualized by UEA-I lectin. (b) Projection image of a time-lapse movie for 4 seconds. Movement of HL-60 cells inside the vascular network was observed. (c) DMSO-induced differentiated HL-60 cells (dHL-60), which mimicked neutrophils, passed through thin vessels with large deformation under the presence of TNFα. (d–f) Representative time-course of extravasation. Extravasation occurred within a short time period (10 min.). Extravasating cells (white arrows) extended protrusions toward the outside of the blood vessel when emigrating from the blood vessel lumen. (g) Three-dimensional structure of extravasated cells (white arrows) shown as max projection x-y and x-z/y-z single slice images. We clearly observed extravasated cells outside of the vasculature. Time separated with colons indicates hours and minutes. Scale bars: 50 μm (a, b); 10 μm (c–g).

https://doi.org/10.1371/journal.pone.0240552.g006

network (Fig 7A). The cells also changed their shape during emigration from the vascular lumen (Fig 7B). We next observed the detailed morphology of cancer cells after extravasation. The emigrated cells maintained adherence to the vascular wall after extravasation and extended protrusions along the endothelial cell surface (Fig 7C–7C"), which may be regarded as filopodia-like protrusions in hematogenous metastasis [30].

Vascularized spheroid culture system with flow

We reproduced the spheroid culture system with perfusable vasculature [15] with a slight modification of the protocol (Fig 8A). First, we produced spheroids using a 96-well plate. Then, the spheroids were embedded in the fibrin gel underneath a glass separator. When we cultured the spheroids for 1 week, HUVECs formed sprouts with a lumen, which were as long

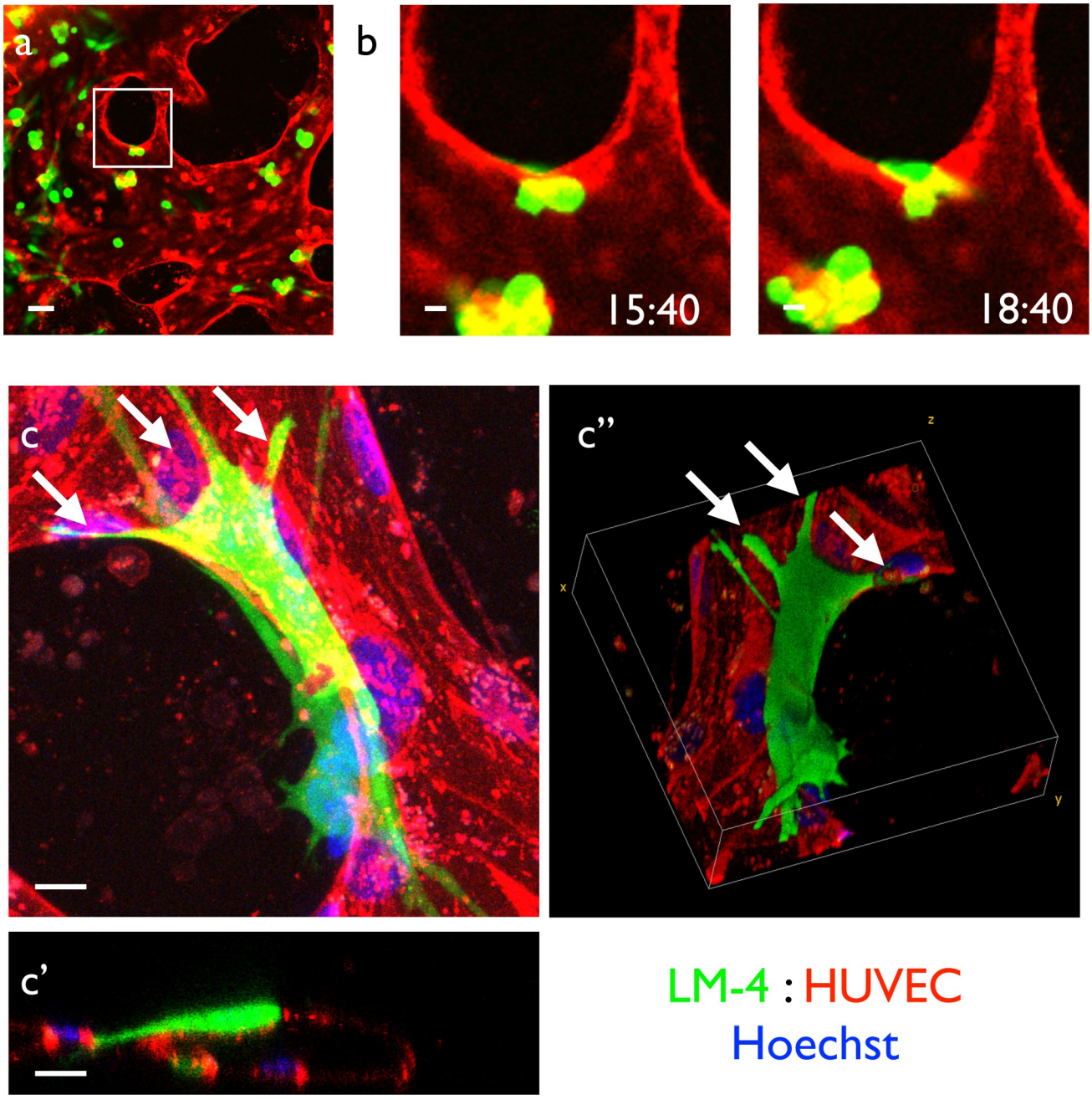

Fig 7. Reproduction of hematogenous metastasis of cancer cells from the capillary network. (a) LM4-GFP cells were introduced into the self-organized capillary network consisting of HUVECs visualized by UEA-1 lectin. (b) High magnification time-lapse view of (a). We observed cancer cells emigrating out of the blood vessels. (c) Detailed morphology of cancer cells on the endothelial cells. Emigrated LM4 cells attached to the blood vessel with highly polarized morphology and multiple protrusions. (c) Max projection image, (c') orthogonal section, and (c'') 3D-reconstructed image. White arrows: cancer cell protrusions. Scale bars: 50 μm (a); 10 μm (b, c).

https://doi.org/10.1371/journal.pone.0240552.g007

as 1 mm (S4 Fig). Then, we cut the tip of the sprouts to perfuse culture medium inside the vascular lumen.

By exerting static pressure between two wells, we observed the medium flow in the connected spheroids (Fig 8B). Interestingly, if we set two spheroids in close vicinity, the vascular sprouts from both spheroids fused and made a serial cluster of spheroids with perfusable vasculature (Fig 8C).

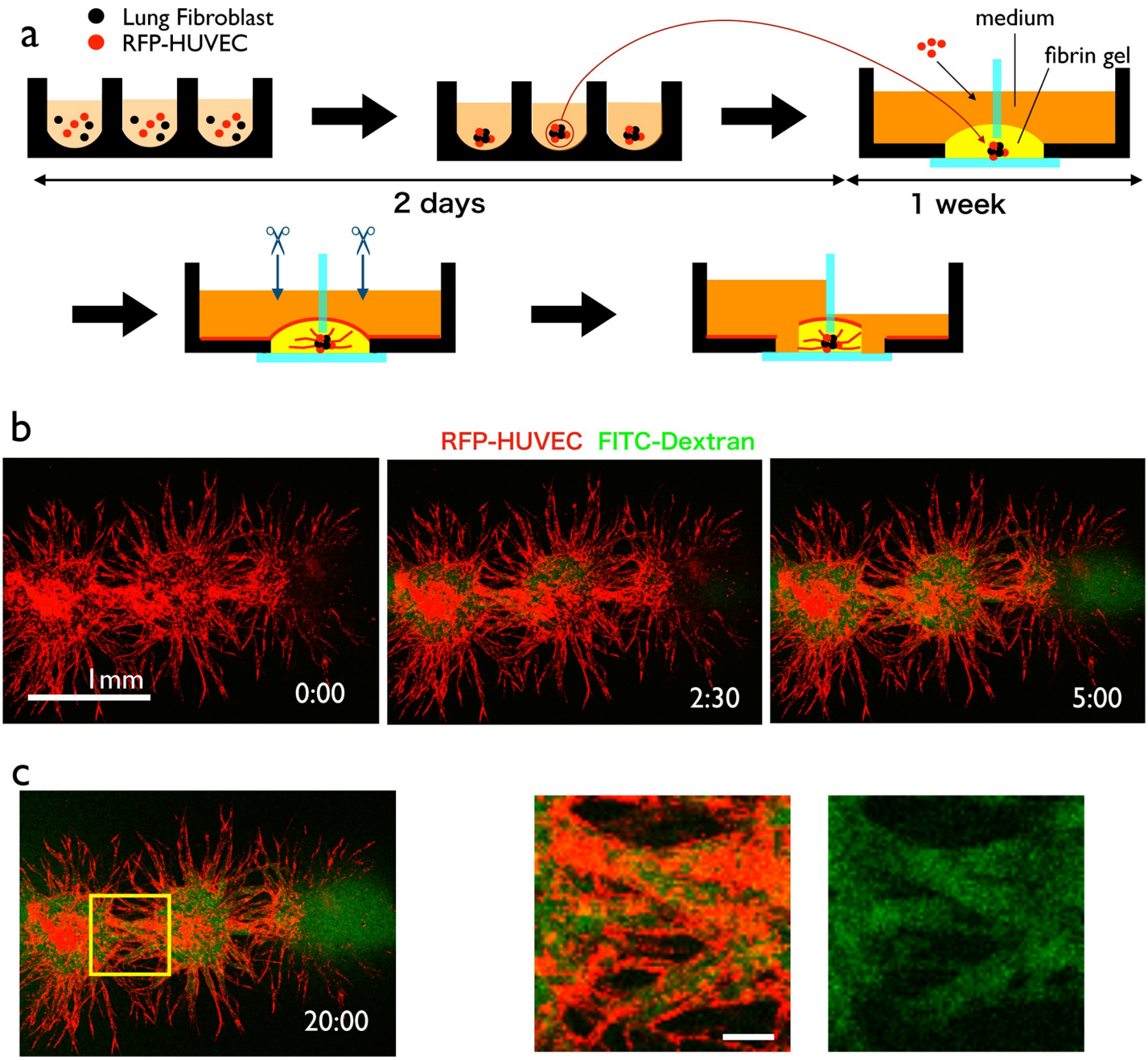

Fig 8. Perfusion of vascularized spheroids. (a) Experimental procedure. Spheroids containing RFP-HUVECs and lung fibroblast were generated and embedded in fibrin gel. After 1 week, sprouts from the spheroids became sufficiently long. Then, we cut the tip of the sprouts from both sides of the well and exerted static pressure to one side of the well. (b) Visualization of the perfusion inside the spheroid using FITC-dextran. (c) High-magnification view of the sprouts connecting two spheroids. FITC-dextran is running through the sprout structure. Scale bar: 1 mm (b); 100 μm (c).

https://doi.org/10.1371/journal.pone.0240552.g008

Discussion

Reconstructive system of pattern formation

In the present study, we constructed a simple perfusion system to reproduce the flow in a capillary network. The seminal work on this type of culture system with flow was performed by Noo-Li Jeon's group [14]. However, the system needs an elaborate microfluidic device that can

only be fabricated by researchers with access to clean room facilities, and it is time consuming for biologists to fully use the system including the device, tubing, and syringe pump. In contrast, our system employs a standard glass-bottom dish without any additional pump, tubing, reservoir, or engineering. The simplicity of the system enabled us to combine it with time-lapse observation on a stage top incubator without any additional apparatus. However, there are several shortcomings because of its simplicity. For example, we could not regulate the flow rate in this system accurately because the driving force for perfusion is static pressure between two wells. For detailed control of flow, we need to use microfluidic devices.

Lumen formation capability of endothelial cells

The mechanism of lumen formation by endothelial cells remains to be elucidated. ECM degradation and apicobasal polarity formation are thought to play a role [31]. In our culture system, one factor was the diffusible signaling molecules from LFs. HUVECs cultivated in fibrin gel formed a network even without LFs, but we could not induce a lumen without coculture with LFs. Two reports used a proteomics approach to identify the diffusible factor responsible for lumen induction by LFs. They identified several factors, but the effect of the combination of these factors was less effective than lung fibroblast coculture [32, 33]. We also found that lumens were preferentially formed at regions near a hard object (S1 Fig). One possible mechanism may be high cell density due to preferential migration of cells toward the hard substrate (durotaxis) [34], but increasing the cell density as a whole did not increase the lumen formation region around hard objects. It was reported that extracellular matrix stiffness promotes lumen formation of endothelial cells [33], which may be related to this tendency. In addition, the lumen formation capacity of HUVECs and LFs differed significantly depending on the production batch. We sometimes experienced HUVECs and LFs whose proliferation appeared to be normal, but lumen formation was poor. Increasing cell numbers sometimes compensated for the low lumen formation activity, but in many cases, using a different batch of cells improved lumen formation.

Effect of the extracellular matrix on the pattern formation mechanism

We used fibrin gel to generate a perfusable vascular network based on a previous study [14]. Fibrin is the main component of a blood clot and not used in physiological tissues. We tried to substitute fibrin gel with other physiological extracellular matrixes such as Matrigel and type I collagen without success. This may be due to the physical viscosity difference. A fibrin gel solution is less viscous than a collagen gel solution. As a result, suspended HUVECs in fibrin gel gathered at the bottom of a dish because of gravity. We succeeded in generating a lumen structure in a type I collagen gel by embedding HUVEC spheroids, indicating that the local cell density may be critically important.

Dynamics of pericytes in the capillary network with flow

For recruitment of pericytes to nascent blood vessels, platelet-derived growth factor B (PDGF-B) produced by tip endothelial cells plays pivotal roles [29, 35]. Notably, tip endothelial cells adjacent to hypoxic tissues are exposed to high concentrations of VEGF-A [35]. Moreover, because of the absence of lumens, tip endothelial cells have limited access to circulating blood [35]. Consistently, cultured HUVECs under high oxygen pressure exhibit reduced production of PDGF-B [36]. In our pericyte-HUVEC coculture with flow, pericytes unexpectedly disappeared in the flow region. A possible reason may be the lack of PDGF-B in the flow region. Endothelial cells in the flow region were under normoxic conditions. There are no flow regions in which endothelial cells should produce PDGF-B [36], and because of the

PDGF-B gradient, pericytes might migrate away from the flow region or extensively proliferate at non-flow regions.

Application of the culture method to embryonic tissues

The final goal of this method is culturing embryonic tissues or organoids with microcirculation, but the connection between two different capillary systems still remains a major challenge. We tried to establish connections between the self-organized HUVEC vascular network and the vascular network in embryonic tissue. The endothelial cells from the embryonic tissue appeared to adhere to the HUVEC structure. However, the lumens of these vasculatures did not form a connection. Therefore, we could not perfuse the vasculature in embryonic tissue (S5 Fig). Additional factors may be necessary to use this culture system as an alternative to organ culture. Because direct connection of two vascular systems is still a major challenge, currently, a technically simpler experimental model of vasculature-blood cell interactions may be a major field of application. In the present study, we demonstrated two applications, dynamics of inflammatory cells and hematogenic metastasis. Various other system can be implemented with our current model without additional costs.

Relationship between microfluidic device methods

This method may be a very good prescreening method for microfluidic device experiments. The major merit of this method is the ease and low cost. We have experienced difficulty in introducing blood vessel into a microfluidic device [15] because it requires specialized skills to connect tubes without damaging gels or endothelial cell networks. As a result, it is difficult to perform a large number of microfluidic device experiments because of its technical difficulty. Although we only used a constant pressure condition for medium perfusion and could not strictly control the flow, this method may be a good starting point to roughly estimate the effect of flow in biological laboratories.

Supporting information

S1 Fig. Lumen formation was observed only around solid objects. (a) Brightfield image of HUVECs cocultured with LFs in fibrin gel in the *periphery* of the dish. A lumen structure was observed. (b) Fluorescence image of HUVECs cocultured with LFs in fibrin gel in the *periphery* of the dish. HUVECs were stained with UEA1-FITC. A lumen structure was observed (white arrows). (c) Brightfield image of HUVECs cocultured with LFs in fibrin gel in the *center* of the dish. A lumen structure was not clear. (d) Fluorescence image of HUVECs cocultured with LFs in fibrin gel in the *center* of the dish. HUVECs were stained with UEA1-FITC. Lumen formation was not clear. (e) Brightfield image of HUVECs cocultured with LFs in fibrin gel near 1 mm glass beads (dashed red circle) *embedded in* the fibrin gel. We observed lumen formation around beads. (f) Confocal image of HUVECs cocultured with LFs in fibrin gel near 1 mm glass beads *embedded in* the fibrin gel. HUVECs were stained with UEA1. We observed lumen formation around beads. (g) Brightfield image of HUVECs cocultured with LFs in fibrin gel near 1 mm glass beads *placed on* the fibrin gel. We observed lumen formation around beads. (h) Confocal image of HUVECs cocultured with LFs in fibrin gel near 1 mm glass beads *placed on* the fibrin gel. HUVECs were stained with UEA1. We observed lumen formation around the beads (asterisks). (i) Three-dimensional structure of RFP-HUVECs around the glass beads. We observed the lumen around beads (asterisks). (j) Scheme of lumen formation region in normal glass-bottom dish and dish with glass separator. Scale bars: 100 μm (a–d, i); 1 mm (e-h).
(PDF)

S2 Fig. Three-dimensional structure of the inlet region on day 21. (a) Brightfield image of the inlet hole region. Arrow: small hole made by fine forceps. (b) Three-dimensional structure of the inlet hole observed by confocal microscopy, basal level. We observe RFP-HUVECs formed the floor of the lumen near the glass bottom. A hole at the ceiling was observed (arrow). (c) Three-dimensional structure of the inlet hole observed by confocal microscopy, middle level. The hole is bordered by RFP-HUVECs (arrow). (d) Three-dimensional structure of the inlet hole observed by confocal microscopy, upper level. The hole was continuous (arrow), and endothelial cells covered the surface of the fibrin gel (arrowheads). Scale bars: 200 μm.
(PDF)

S3 Fig. Effect of flow on the self-organized endothelial cell network with pericytes. (a) Low magnification view at day 0. Locations of the inlet and outlet are shown by white arrows. (b) Low magnification view at day 21. (c) Confirmation of perfusion at day 30. GFP-pericytes were labeled green. Endothelial cells were stained with UEA-1 lectin (red). Characteristics of the vessel shape were similar to that without pericytes. (d) Three-dimensional view of the vasculature. We perfused culture medium with FITC-dextran (green) and did not observe leakage. (e) Histological observation of the flow region. (f) Histological observation of the low flow region. (g) High magnification view of the cyst structure in the non-flow region. (h) Histological structure of pericytes within a gel in the non-flow region. (i) TUNEL staining of the flow region. No dead cells were observed. (j) TUNEL staining of the non-flow region. A positive signal was observed within the cyst. (k) Type IV collagen (T4C) staining near the cyst. A large ECM sheath structure was observed (arrowhead) near the cyst (arrow). (l) Type IV collagen and desmin staining of the non-flow region. Desmin-positive pericytes were observed within the gel, which colocalized with type IV collagen. Scale bars: 3 mm (a, b); 1 mm (c); 250 μm (d);100 μm (e-l).
(PDF)

S4 Fig. Quantification of the sprout length from endothelial cell-containing spheroids. (a) Spheroids containing RFP-HUVECs were cultivated for 2 days in a culture plate and then transferred to fibrin gel. (b) The length of angiogenic sprouts from the centroid of the fluorescent signal was measured every day. The length of the sprout became saturated after 7 days, and the radius was around 1 mm, which enabled us to directly cut the tip of the sprout to generate an open end.
(PDF)

S5 Fig. Attempt to connect vasculature to the embryonic tissue. (a) E12 mouse embryonic kidney tissue was dissected, and the central one-third of the kidney was embedded in fibrin gel. The tissue was sandwiched by two RFP-HUVEC:hLF spheroids. (b) After 1 week, HUVEC-LF spheroids generated sprouts towards the embryonic kidney tissue. (c) Sprouts from RFP-HUVECs appeared to avoid the embryonic tissue. (c') 3D observation of HUVECs and mouse endothelial cells revealed that, although mouse endothelial cells (green) tended to attach to RFP-HUVECs, they did not connect vasculature with lumens together. (d) Histological observation of the cultured tissue. Kidney explants formed collecting tubule-like structures, but the endothelial sprouts from the HUVEC spheroids did not form a connection with the kidney structure.
(PDF)

S1 Movie. Flow of fluorescent particles in the self-organized capillary network. Real-time movie of fluorescent particles flowing in a self-organizing vascular network in fibrin gel.
(AVI)

S2 Movie. Flow of red blood cells in the self-organized capillary network. Real-time movie of red blood cell flowing in a self-organized vascular network in fibrin gel. Blood was diluted 20× using EGM-2 and loaded on one side of the well (Fig 1L and 1M).
(AVI)

S3 Movie. Cell debris flowing during the medium change (long-term perfusion experiment). Real-time movie of cell debris flowing in a self-organized vascular network in fibrin gel during the long-term perfusion experiment (Fig 2). We confirmed perfusion during the medium change process.
(AVI)

S4 Movie. Collective migration of endothelial cells. Time-lapse movie of the flow region in the long-term flow experiment (Fig 2A–2C). The stream-like movement of endothelial cells was observed in the opposite direction to flow. Frame rate: 3 min/frame, 180 min.
(TIF)

S5 Movie. Dilation of the vessels in the flow region. Time-lapse movie of the flow region in the long-term flow experiment (Fig 3A). The vessel with flow was maintained alive, and some vessels became dilated. Frame rate: 1 day/frame, 30 days.
(AVI)

S6 Movie. Disappearance of unused vessels in the non-flow region. Time-lapse movie of the non-flow region in the long-term flow experiment (Fig 3B). The vessel became disconnected and degraded gradually. Frame rate: 1 day/frame, 30 days.
(AVI)

S7 Movie. Movement of pericytes in the flow region. Time-lapse movie of pericytes (green) in the flow region (upper half) and non-flow region (lower half). In the flow region, the pericytes simply disappeared, whereas in the non-flow region, pericytes proliferated extensively.
(AVI)

S8 Movie. Flow of HL60 cells in the self-organized vascular network. Time-lapse movie of HL60 (green) in HUVEC-RFP vascular network.
(AVI)

Acknowledgments

The authors thank Professor Fumio Arai for helpful suggestions. We also thank Mitchell Arico from Edanz Group (https://en-author-services.edanzgroup.com/) for editing a draft of this manuscript.

Author Contributions

Conceptualization: Sanshiro Hanada, Takashi Miura.

Data curation: Yoshimi Yamaguchi, Yuji Nashimoto, Takashi Miura.

Investigation: Kei Sugihara, Yoshimi Yamaguchi, Shiori Usui, Yuji Nashimoto, Ryuji Yokokawa, Koichi Nishiyama, Takashi Miura.

Methodology: Yoshimi Yamaguchi, Shiori Usui, Sanshiro Hanada, Akiyoshi Uemura, Ryuji Yokokawa, Koichi Nishiyama, Takashi Miura.

Project administration: Takashi Miura.

Resources: Yoshimi Yamaguchi, Sanshiro Hanada, Etsuko Kiyokawa, Akiyoshi Uemura.

Supervision: Sanshiro Hanada, Etsuko Kiyokawa, Akiyoshi Uemura, Ryuji Yokokawa, Koichi Nishiyama.

Validation: Etsuko Kiyokawa, Ryuji Yokokawa.

Visualization: Yoshimi Yamaguchi, Shiori Usui, Yuji Nashimoto, Takashi Miura.

Writing – original draft: Kei Sugihara, Takashi Miura.

Writing – review & editing: Takashi Miura.

References

1. Gilbert SF, Michael J. Barresi. Developmental Biology. 11th ed. Sinauer; 2018.
2. Wolpert L, Tickle C. Principles of development. 4th ed. New York, New York, USA: Oxford University Press; 2011.
3. Sadler TW. Langman's Medical Embryology. 10th ed. Baltimore: Lippincott Williams & Wilkins; 2006. https://doi.org/10.1097/00006534-198801000-00024
4. Shamir ER, Ewald AJ. Three-dimensional organotypic culture: Experimental models of mammalian biology and disease [Internet]. Nature Reviews Molecular Cell Biology. 2014. pp. 647–664. https://doi.org/10.1038/nrm3873 PMID: 25237826
5. Clevers H. Modeling Development and Disease with Organoids. Cell. 2016; 165: 1586–1597. https://doi.org/10.1016/j.cell.2016.05.082 PMID: 27315476
6. Miura T, Yokokawa R. Tissue culture on a chip: Developmental biology applications of self-organized capillary networks in microfluidic devices. Dev Growth Differ. 2016; 58: 505–515. https://doi.org/10.1111/dgd.12292 PMID: 27272910
7. Auger FA, Gibot L, Lacroix D. The Pivotal Role of Vascularization in Tissue Engineering. Annu Rev Biomed Eng. 2013; 15: 177–200. https://doi.org/10.1146/annurev-bioeng-071812-152428 PMID: 23642245
8. Kubota Y, Kleinman HK, Martin GR, Lawley TJ. Role of laminin and basement membrane in the morphological differentiation of human endothelial cells into capillary-like structures. J Cell Biol. 1988; 107: 1589–1598. https://doi.org/10.1083/jcb.107.4.1589 PMID: 3049626
9. Armulik A, Abramsson A, Betsholtz C. Endothelial/pericyte interactions. Circ Res. 2005; 97: 512–523. https://doi.org/10.1161/01.RES.0000182903.16652.d7 PMID: 16166562
10. Wagner DD, Frenette PS. The vessel wall and its interactions. Blood. 2008; 111: 5271–5281. https://doi.org/10.1182/blood-2008-01-078204 PMID: 18502843
11. Williams MR, Azcutia V, Newton G, Alcaide P, Luscinskas FW. Emerging mechanisms of neutrophil recruitment across endothelium [Internet]. Trends in Immunology. 2011. pp. 461–469. https://doi.org/10.1016/j.it.2011.06.009 PMID: 21839681
12. Gupta GP, Massagué J. Cancer Metastasis: Building a Framework [Internet]. Cell. 2006. pp. 679–695. https://doi.org/10.1016/j.cell.2006.11.001 PMID: 17110329
13. Song HHG, Rumma RT, Ozaki CK, Edelman ER, Chen CS. Vascular Tissue Engineering: Progress, Challenges, and Clinical Promise. Cell Stem Cell. 2018; 22: 340–354. https://doi.org/10.1016/j.stem.2018.02.009 PMID: 29499152
14. Kim S, Lee H, Chung M, Jeon NL. Engineering of functional, perfusable 3D microvascular networks on a chip. Lab Chip. 2013; 13: 1489–1500. https://doi.org/10.1039/c3lc41320a PMID: 23440068
15. Nashimoto Y, Hayashi T, Kunita I, Nakamasu A, Torisawa YS, Nakayama M, et al. Integrating perfusable vascular networks with a three-dimensional tissue in a microfluidic device. Integr Biol. 2017; 9: 506–518. https://doi.org/10.1039/C7IB00024C PMID: 28561127
16. Nashimoto Y, Okada R, Hanada S, Arima Y, Nishiyama K, Miura T, et al. Vascularized cancer on a chip: The effect of perfusion on growth and drug delivery of tumor spheroid. Biomaterials. 2020; 229: 119547. https://doi.org/10.1016/j.biomaterials.2019.119547 PMID: 31710953
17. Zervantonakis IK, Hughes-Alford SK, Charest JL, Condeelis JS, Gertler FB, Kamm RD. Three-dimensional microfluidic model for tumor cell intravasation and endothelial barrier function. Proc Natl Acad Sci. 2012; 109: 13515–13520. https://doi.org/10.1073/pnas.1210182109 PMID: 22869695

18. Chen MB, Whisler JA, Jeon JS, Kamm RD. Mechanisms of tumor cell extravasation in an in vitro microvascular network platform. Integr Biol (United Kingdom). 2013; 5: 1262–1271. https://doi.org/10.1039/c3ib40149a PMID: 23995847

19. Chen MB, Whisler JA, Fröse J, Yu C, Shin Y, Kamm RD. On-chip human microvasculature assay for visualization and quantification of tumor cell extravasation dynamics. Nat Protoc. 2017; 12: 865–880. https://doi.org/10.1038/nprot.2017.018 PMID: 28358393

20. van Duinen V, Zhu D, Ramakers C, van Zonneveld AJ, Vulto P, Hankemeier T. Perfused 3D angiogenic sprouting in a high-throughput in vitro platform. Angiogenesis. 2019; 22: 157–165. https://doi.org/10.1007/s10456-018-9647-0 PMID: 30171498

21. Nakatsu MN, Sainson RCA, Aoto JN, Taylor KL, Aitkenhead M, Pérez-del-Pulgar S, et al. Angiogenic sprouting and capillary lumen formation modeled by human umbilical vein endothelial cells (HUVEC) in fibrin gels: The role of fibroblasts and Angiopoietin-1. Microvasc Res. 2003; 66: 102–112. https://doi.org/10.1016/s0026-2862(03)00045-1 PMID: 12935768

22. Corbett TH, Griswold DP, Roberts BJ, Peckham JC, Schabel FM. Tumor Induction Relationships in Development of Transplantable Cancers of the Colon in Mice for Chemotherapy Assays, with a Note on Carcinogen Structure. Cancer Res. 1975; 35: 2434–2439. PMID: 1149045

23. Schneider CA, Rasband WS, Eliceiri KW. NIH Image to ImageJ: 25 years of image analysis. Nat Methods. 2012; https://doi.org/10.1038/nmeth.2089 PMID: 22930834

24. Schindelin J, Arganda-Carreras I, Frise E, Kaynig V, Longair M, Pietzsch T, et al. Fiji: An open-source platform for biological-image analysis. Nat Methods. 2012; 9: 676–682. https://doi.org/10.1038/nmeth.2019 PMID: 22743772

25. Sato Y, Poynter G, Huss D, Filla MB, Czirok A, Rongish BJ, et al. Dynamic analysis of vascular morphogenesis using transgenic quail embryos. PLoS One. 2010; 5: 1–12. https://doi.org/10.1371/journal.pone.0012674 PMID: 20856866

26. Ostrowski MA, Huang NF, Walker TW, Verwijlen T, Poplawski C, Khoo AS, et al. Microvascular endothelial cells migrate upstream and align against the shear stress field created by impinging flow. Biophys J. 2014; 106: 366–374. https://doi.org/10.1016/j.bpj.2013.11.4502 PMID: 24461011

27. Hsu PP, Li S, Li YS, Usami S, Ratcliffe A, Wang X, et al. Effects of flow patterns on endothelial cell migration into a zone of mechanical denudation. Biochem Biophys Res Commun. 2001; 285: 751–759. https://doi.org/10.1006/bbrc.2001.5221 PMID: 11453657

28. Sakaue-Sawano A, Kurokawa H, Morimura T, Hanyu A, Hama H, Osawa H, et al. Visualizing Spatiotemporal Dynamics of Multicellular Cell-Cycle Progression. Cell. 2008; 132: 487–498. https://doi.org/10.1016/j.cell.2007.12.033 PMID: 18267078

29. Uemura A, Ogawa M, Hirashima M, Fujiwara T, Koyama S, Takagi H, et al. Recombinant angiopoietin-1 restores higher-order architecture of growing blood vessels in mice in the absence of mural cells. J Clin Invest. 2002; 110: 1619–1628. https://doi.org/10.1172/JCI15621 PMID: 12464667

30. Shibue T, Brooks MW, Fatih Inan M, Reinhardt F, Weinberg RA. The outgrowth of micrometastases is enabled by the formation of filopodium-like protrusions. Cancer Discov. 2012; 2: 706–721. https://doi.org/10.1158/2159-8290.CD-11-0239 PMID: 22609699

31. Davis GE, Stratman AN, Sacharidou A, Koh W. Molecular Basis for Endothelial Lumen Formation and Tubulogenesis During Vasculogenesis and Angiogenic Sprouting. International Review of Cell and Molecular Biology. 2011. pp. 101–165. https://doi.org/10.1016/B978-0-12-386041-5.00003-0 PMID: 21482411

32. Newman AC, Chou W, Welch-Reardon KM, Fong AH, Popson SA, Phan DT, et al. Analysis of stromal cell secretomes reveals a critical role for stromal cell-derived hepatocyte growth factor and fibronectin in angiogenesis. Arterioscler Thromb Vasc Biol. 2013; 33: 513–522. https://doi.org/10.1161/ATVBAHA.112.300782 PMID: 23288153

33. Newman AC, Nakatsu MN, Chou W, Gershon PD, Hughes CCW. The requirement for fibroblasts in angiogenesis: fibroblast-derived matrix proteins are essential for endothelial cell lumen formation. Mol Biol Cell. 2011; 22: 3791–3800. https://doi.org/10.1091/mbc.E11-05-0393 PMID: 21865599

34. Sunyer R, Conte V, Escribano J, Elosegui-Artola A, Labernadie A, Valon L, et al. Collective cell durotaxis emerges from long-range intercellular force transmission. Science (80-). 2016; 353: 1157–1161. https://doi.org/10.1126/science.aaf7119 PMID: 27609894

35. Gerhardt H, Golding M, Fruttiger M, Ruhrberg C, Lundkvist A, Abramsson A, et al. VEGF guides angiogenic sprouting utilizing endothelial tip cell filopodia. J Cell Biol. 2003; 161: 1163–1177. https://doi.org/10.1083/jcb.200302047 PMID: 12810700

36. Kourembanas S, Hannan RL, Faller D V. Oxygen tension regulates the expression of the platelet-derived growth factor-B chain gene in human endothelial cells. J Clin Invest. 1990; 86: 670–674. https://doi.org/10.1172/JCI114759 PMID: 2384608